# Investigation into how the magnesia, silica, and alumina contents of iron ore sinter influence its mineralogy and properties

by M.K. Kalenga* and A.M. Garbers-Craig†


## Synopsis

The influence of varying amounts of magnesia, silica, and alumina in iron ore sinter on its mineralogy, reducibility index (RI), reduction disintegration index (RDI), physical breakdown (AI and TI), and production properties (coke breeze rate) were examined.

It was found that the mineralogy of iron sinter can more easily be predicted from its chemical composition than from the RI, RDI, AI or TI. Anticipating the consequence that varying amounts of MgO and $SiO_2$ would have on sinter properties is complex, and not necessarily predictable. High concentrations of $Al_2O_3$ in the sinter result in high concentrations of the SFCA phase, but with drastically deteriorated properties. This study also confirmed that the form in which fluxes are added to the raw material sinter mixture affects the mineralogy and properties of the produced sinter.



**Keywords**
Iron sinter, mineralogy, reducibility, reduction degradation, abrasion index, tumble index.


## Introduction

The structure of iron ore sinter is not uniform. It consists of pores (of varying sizes) and a complex aggregate of phases, each with different properties. It is the combination of these pores and phases, and the interaction between them that determines the sinter properties, but also makes the prediction of sinter properties so difficult[1,2]. Various studies are reported in the literature in which correlations are drawn between raw material composition (such as phosphorous, silica, alumina and magnesia contents, sinter basicity, melt fluidity, $Al_2O_3/SiO_2$ ratio, $TiO_2$ contents), porosity, maximum sintering temperature, as well as the structure and properties of iron sinter[3–12]. Alternative raw materials that can be used in the sinter mixture have also been tested, and their impact on sinter quality evaluated[13,14]. Despite all the research done, the correlation between the chemical composition and mineralogy of iron sinter and its properties and behaviour are still not clearly understood. This paper therefore reports on a further investigation into the effect of varying MgO, $SiO_2$ and $Al_2O_3$ contents of iron ore sinter on its chemical and physical properties.

## Background

Iron ore fines cannot directly be charged into the blast furnace, as they are detrimental to the permeability of the furnace, and can also be lost in the top gas. These fines are therefore agglomerated into larger pieces, of which one type of agglomeration process is sintering. Many reactions may take place during the sintering process. Equilibrium phase relations are however not reached during sintering, due to the flame front that rapidly passes through the sinter bed. This results in the high degree of heterogeneity of the sinter, and the formation of non-equilibrium phases that are not expected from thermodynamic considerations. The composition of the sinter therefore varies from place to place in the bulk material, depending on the nature of the individual ore and flux particles and the extent of reactions between them[15]. Macroscopically iron sinter has a non-uniform structure with large irregular pores. Microscopically it consists of bonding phases, relict ore particles, remaining glassy phases and very small non-uniform pores and cracks. Depending on different parameters such as temperature, composition, oxygen partial pressure, time and atmosphere, different phases form in different proportions, while different morphologies develop[15]. The morphology essentially reflects the mode of formation and is related to a particular chemical composition, heating and cooling rate of the sinter. Some of the common minerals and phases present in iron ore sinter are hematite ($Fe_2O_3$), magnetite ($Fe_3O_4$),


* *Department of Extraction Metallurgy, Faculty of Engineering, the Built Environment, University of Johannesburg, South Africa.*

† *Department of Materials Science and Metallurgical Engineering, Faculty of Engineering, the Built Environment and Information Technology, University of Pretoria, South Africa.*


 *SA ISSN 0038–223X/3.00 + 0.00. Paper received Nov. 2008; revised paper received Jun. 2010.*

magnesioferrite $(Mg,Fe)_3O_4$, silicoferrite of calcium and alumina (SFCA), with stoichiometries $M_{14+6n}O_{20+8n}$ and $M_{25}O_{36}$, where n=0,1 and M= Ca, Fe, Al, Si), anorthite ($CaAl_2Si_2O_8$), calcium diferrite ($CaFe_4O_7$), dicalcium ferrite ($Ca_2(Fe,Al)_2O_5$), dicalcium silicate ($Ca_2SiO_4$), $SiO_2$-rich glass, free lime, periclase (MgO) and olivine $(Mg,Fe)_2SiO_4$[15].

Sinter quality is defined as a combination of its cold strength, its degradation during reduction at low temperatures, its reducibility and its high temperature properties that are related to the temperatures at which the sinter starts to soften, melt and drip during reduction at temperatures above1150°C. All of these properties, which are evaluated according to standardized tests, are strongly related to the mineralogy, microscopic and macroscopic structure of the sinter[16]. The reproducibility of these tests that are performed on sinter particles to evaluate their quality is therefore low in comparison with that of synthetic samples due to the high degree of variability in phase composition between sinter particles, even when these sinter particles are obtained from the same bulk material[17].

## Experimental

### *Preparation of sinter samples*

Sinter mixtures constituted from South African iron ores (Sishen and Thabazimbi), fluxes (dolomite and lime), coke as well as return fines were used. The MgO content of the sinter was varied through the addition of either dolomite or fused magnesia, whereas the alumina content was increased through the addition of bauxite. The basicities (mass per cent CaO/mass per cent $SiO_2$) of the sinters ranged between 1.8 and 1.95, with a FeO content that ranged between 7.0–9.0 mass per cent. The sinter experiments were performed in a sinter pot at the pilot plant of Kumba Iron Ore (Pretoria West, South Africa). The raw materials were weighed into the required proportions, mixed dry in a rotary drum mixer, after which 5.1 mass per cent water and 0.7 mass per cent $FeCl_3$ were added and mixing continued for a further six minutes. After mixing, the raw materials were fed into the sinter pot via a conveyor belt onto a grid layer, which consisted of –40 mm +20 mm sinter particles, 50 mm in height. The bed was ignited at 1050°C, using a gas flame.

The following types of sinters were produced: low silica—low alumina sinters (5.1 mass per cent $SiO_2$–1.6 mass per cent $Al_2O_3$) with MgO contents of 1, 2, and 2.8 mass per cent respectively that were adjusted through the addition of dolomite (Table I); high silica—low alumina sinters (5.6 mass per cent $SiO_2$–1.7 mass per cent $Al_2O_3$) with MgO contents of 1, 1.8, and 2.8 mass per cent respectively, that were adjusted through the addition of either dolomite or fused magnesia (Tables II and III), and a high silica—high alumina (5.8 mass per cent $SiO_2$—2.9 mass per cent $Al_2O_3$) sinter with a MgO content of 2.6 mass per cent, that was obtained through the addition of dolomite (Table IV).

*Table I*

**Chemical compositions of the low silica-low alumina sinter (mass%)**

| Compound | | $Fe_{(total)}$ | FeO | $Fe_2O_3$ | Fe(met) | CaO | MgO | $SiO_2$ | $Al_2O_3$ | $K_2O$ | $Na_2O$ | $TiO_2$ |
|---|---|---|---|---|---|---|---|---|---|---|---|---|
| MgO | 1 | 57.6 | 8.0 | 73.2 | 0.13 | 9.6 | 1.2 | 5.0 | 1.7 | 1.0 | 0.0 | 0.1 |
| | 2 | 58.0 | 7.9 | 74 | 0.12 | 9.8 | 2.0 | 5.1 | 1.7 | 0.0 | 0.0 | 0.1 |
| | 2.8 | 56.1 | 8.1 | 71.1 | 0.0 | 10.3 | 2.8 | 5.2 | 1.3 | 0.0 | 0.0 | 0.1 |

*Table II*

**Chemical compositions of the high silica-low alumina sinter, with dolomite addition (mass %)**

| Composition | 1% MgO | | | 2% MgO | | | 3% MgO | | |
|---|---|---|---|---|---|---|---|---|---|
| | Sample 1 | Sample 2 | Average | Sample 3 | Sample 4 | Average | Sample 5 | Sample 6 | Average |
| $Fe_{(total)}$ | 58.80 | 57.10 | 57.95 | 56.60 | 55.90 | 56.25 | 55.70 | 55.20 | 55.45 |
| FeO | 7.70 | 8.14 | 7.92 | 7.98 | 8.01 | 8.00 | 7.12 | 7.89 | 7.51 |
| $Fe_2O_3$ | 72.50 | 72.40 | 72.45 | 71.64 | 70.64 | 71.14 | 71.72 | 71.10 | 70.41 |
| $Fe_{(met)}$ | 0.10 | 0.11 | 0.11 | 0.29 | 0.27 | 0.28 | 0.01 | 0.05 | 0.03 |
| CaO | 10.50 | 10.20 | 10.35 | 10.20 | 10.70 | 10.45 | 11.20 | 11.00 | 11.10 |
| MgO | 1.10 | 1.14 | 1.12 | 1.65 | 1.94 | 1.80 | 2.92 | 2.71 | 2.82 |
| $SiO_2$ | 5.76 | 5.69 | 5.73 | 5.60 | 5.77 | 5.69 | 5.80 | 5.57 | 5.69 |
| $Al_2O_3$ | 1.70 | 1.68 | 1.69 | 1.67 | 1.68 | 1.68 | 1.73 | 1.69 | 1.71 |
| $K_2O$ | 0.06 | 0.06 | 0.06 | 0.05 | 0.04 | 0.05 | 0.04 | 0.05 | 0.04 |
| $Na_2O$ | 0.01 | 0.01 | 0.01 | 0.01 | 0.01 | 0.01 | 0.01 | 0.01 | 0.01 |
| $TiO_2$ | 0.10 | 0.10 | 0.10 | 0.10 | 0.10 | 0.10 | 0.11 | 0.10 | 0.10 |
| MnO | 0.32 | 0.31 | 0.31 | 0.32 | 0.32 | 0.32 | 0.35 | 0.14 | 0.35 |
| P | 0.05 | 0.04 | 0.04 | 0.04 | 0.04 | 0.04 | 0.04 | 0.05 | 0.05 |
| S | 0;01 | 0.01 | 0.01 | 0.02 | 0.01 | 0.01 | 0.01 | 0.01 | 0.01 |
| C | 0.08 | 0.06 | 0.07 | 0.15 | 0.14 | 0.16 | 0.28 | 0.28 | 0.28 |
| Basicity | 1.82 | 1.79 | 1.81 | 1.82 | 1.85 | 1.84 | 1.93 | 1.97 | 1.95 |

*Table III*

**Chemical compositions of the high silica-low alumina sinter, with fused magnesia addition (mass %)**

| Composition | 1% MgO | | | 2% MgO | | | 3% MgO | | |
|---|---|---|---|---|---|---|---|---|---|
| | Sample 1 | Sample 2 | Average | Sample 3 | Sample 4 | Average | Sample 5 | Sample 6 | Average |
| $Fe_{(total)}$ | 56.40 | 56.70 | 56.55 | 56.80 | 55.70 | 56.55 | 55.7 | 55.40 | 55.60 |
| FeO | 8.21 | 7.36 | 7.72 | 7.45 | 7.36 | 7.41 | 8.00 | 7.64 | 7.80 |
| $Fe_2O_3$ | 71.60 | 72.80 | 72.15 | 72.70 | 72.20 | 72.45 | 70.5 | 70.60 | 70.6 |
| $Fe_{(met)}$ | 0.05 | 0.07 | 0.06 | 0.17 | 0.20 | 0.19 | 0.21 | 0.65 | 0.10 |
| CaO | 11.20 | 11.00 | 11.10 | 10.90 | 10.50 | 10.70 | 10.08 | 11.00 | 10.9 |
| MgO | 1.00 | 1.00 | 1.00 | 1.36 | 1.75 | 1.56 | 2.50 | 2.80 | 2.70 |
| $SiO_2$ | 5.79 | 5.54 | 5.67 | 5.44 | 5.54 | 5.49 | 5.65 | 5.47 | 5.56 |
| $Al_2O_3$ | 1.75 | 1.71 | 1.73 | 1.64 | 1.67 | 1.66 | 1.70 | 1.65 | 1.70 |
| $K_2O$ | 0.07 | 0.07 | 0.07 | 0.06 | 0.10 | 0.08 | 0.07 | 0.08 | 0.08 |
| $Na_2O$ | 0.01 | 0.01 | 0.01 | 0.01 | 0.01 | 0.01 | 0.01 | 0.02 | 0.01 |
| $TiO_2$ | 0.10 | 0.10 | 0.10 | 0.09 | 0.10 | 0.09 | 0.11 | 0.10 | 0.10 |
| MnO | 0.31 | 0.28 | 0.29 | 0.29 | 0.30 | 0.30 | 0.40 | 0.14 | 0.35 |
| P | 0.08 | 0.04 | 0.06 | 0.04 | 0.05 | 0.05 | 0.04 | 0.05 | 0.05 |
| S | 0.01 | 0.02 | 0.01 | 0.02 | 0.01 | 0.02 | 0.01 | 0.01 | 0.01 |
| C | 0.25 | 0.19 | 0.22 | 0.60 | 0.17 | 0.12 | 0.28 | 0.28 | 0.28 |
| Basicity | 1.82 | 1.79 | 1.81 | 2.00 | 1.90 | 1.95 | 1.93 | 1.97 | 1.95 |

*Table IV*

**Chemical composition of the high silica-high alumina sinter (mass%)**

| $Fe_{(tot)}$ | FeO | $Fe_2O_3$ | Fe(met) | CaO | MgO | $SiO_2$ | $Al_2O_3$ | $K_2O$ | $Na_2O$ | $TiO_2$ | MnO | P | S | C | Basicity |
|---|---|---|---|---|---|---|---|---|---|---|---|---|---|---|---|
| 54.9 | 7.9 | 69.6 | 0.1 | 10.7 | 2.6 | 5.8 | 2.9 | 0.0 | 0.0 | 0.3 | 0.0 | 0.0 | 0.0 | 0.0 | 1.9 |

### *Evaluation of sinter properties*

The produced sinters were evaluated for their mineralogy, reducibility index (RI), reduction disintegration index (RDI), tumbler index (TI), abrasion index (AI), and coke breeze rate, according to ISO specifications.

The mineralogical analysis involved the quantification of phases of different morphologies by point counting. During point counting at least hundred points per sample were counted. Each sample was counted three times, and average values are reported.

The reducibility and therefore reducibility index (RI) depends on the ease with which the reduction gases can penetrate the sinter. Reducibility of the sinter therefore depends on the pore and surface structure, the intrinsic reducibility of the minerals and their assemblages, and the additional surface area generated during reduction as a result of the inherent volumetric changes that take place.

In the upper part of the blast furnace shaft, the permeability of the burden may be influenced by the breakdown of sinter upon reduction. The reduction disintegration index (RDI) is defined as a quantitative measure of the disintegration of the sinter that could occur in the upper part of the blast furnace after some reduction. Sinter with a high degree of reduction disintegration generates fines in the top of the furnace which affects the flow distribution within the blast furnace.

During transportation and charging of sinter into the blast furnace breakdown of the sinter must be minimized. This breakdown is related to its cold strength and evaluated in terms of its tumble (TI) and abrasion indexes (AI).

For each sinter composition the RI, RDI, AI, TI and coke breeze rate of two sets of samples were determined. The following test procedures were followed:

#### *Reducibility index*

The reducibility index (RI) was evaluated according to the ISO 4695:1995(E) test. In this test a fixed bed of sinter particles is reduced isothermally at 950°C, using a reducing gas composition consisting of 40% v/v of CO and 60% v/v of N2. The test portion is weighed at specified time intervals and the weight loss is calculated.

#### *Reduction disintegration index*

The RDI of the sinter was evaluated by using the ISO 4696-1 (1996E) test. During this test sinter of specified size range is subjected to static reduction for 1 hour at a temperature of 500°C using a reducing gas consisting of:

- CO: 20 % (V/V) ± 0.5 %(V/V)
- $CO_2$: 20% (V/V) ± 0.5% (V/V)
- $H_2$: 2.0% (V/V) ± 0.5 % (V/V)
- $N_2$: 58% (V/V) ± 0.5% (V/V).

The test portion is cooled to a temperature below 100°C and tumbled using a drum of 130 mm (inner diameter), for 300 revolutions. The test portion is then sieved, and the reduction disintegration index (RDI) is calculated according to:

- $RDI_{+6.3} = (m_1/ m_0) \times 100$
- $RDI_{-3.15} = (\{m_0 - (m_1 + m_2)/ m_0\}) \times 100$
- $RDI_{-0.5} = (\{m_0 - (m_1 + m_2 + m_3)\}/ m_0) \times 100$

where

$m_0$ = mass in grams of the test portion after reduction and before tumbling

$m_{1,2,3}$ = mass in grams of the oversized fraction retained on the 6.30, 3.15 and 0.5 sieves respectively.

*Tumble and abrasion indexes*

The AI and TI indexes were evaluated by using the ISO 3271 (1995 E) test, where 15 kg of sinter was tumbled at 25 r/ min for 200 revolutions, in a circular drum with internal diameter of 1000 mm and internal length of 500. The tumble index (TI) and abrasion index (AI) are subsequently calculated from a sieve analysis according to:

$$TI = (m_1 / m_0) \times 100$$

$$AI = (\{m_0 - (m_1 + m_2)\}/ m_0) \times 100$$

where:

$m_0$ = mass of the test portion, in kg, weighed and placed in the tumble drum

$m_1$ = mass of + 6.30 mm portion of the tumbled sinter, in kg

$m_2$ = mass of – 6.30 mm + 0.5 mm portion of the tumbled sinter, in kg.

## Results

### *Low silica-low alumina sinter*

*Mineralogy*

The phase compositions of the low silica-low alumina sinters, as determined through point counting, are given in Table V.

From the mineralogy, it can be seen that the volume percentage of the spinel phase ($(Fe^{2+},Mg)(Fe^{3+})O_4$) increased with increasing MgO content in the sinter mix. The total amount of haematite, primary or relict haematite as well as the secondary rhombic haematite decreased, whereas the tertiary or late stage haematite increased with increasing MgO content in the sinter. The total amount of haematite decreased. The amount of magnesio-wustite ((Fe,Mg)O) increased with increasing MgO.

The total amount of silicoferrites of calcium and aluminum (SFCA), the acicular, columnar and blocky SFCA, as well as the ratio of acicular SFCA: columnar SFCA decreased with an increase in MgO content of the sinter. Only the amounts of the dendritic and eutectic SFCA phases increased with an increase in the MgO content of the sinter.

The crystalline silicates decreased, while the amount of glass increased with an increase in MgO content.

*Sinter properties*

The reducibility index decreased with an increase in MgO content (Figure 1). Both the RDI (+3.15 mm) and RDI (+6.3 mm) decreased when MgO was increased from 1 to 2 per cent MgO, after which it increased with a further addition of MgO to 2.8 mass per cent MgO (Figures 2a and 2b). The abrasion index increased with increasing MgO content of the sinter (Figure 3), while the trend of the tumble index with increasing MgO content seems to be similar although the value of the TI has a high degree of uncertainty at a MgO content of 2.8 per cent MgO (Figure 4).

The coke breeze rate increased with increasing MgO content (Figure 5). It can be assumed that this is due to the fact that the MgO was increased through dolomite addition, and that more energy was required for carbonate decomposition, as well as the dehydration of any $Ca(OH)_2$ and $Mg(OH)_2$ that could have formed after carbonate decomposition.

*Table V*

**Quantification of phases in the low silica-low alumina sinter (volume %)**

| Phase | MgO added (mass %) | | |
|---|---|---|---|
| | 1.2 | 2.0 | 2.8 |
| Spinel | 32.5 ± 0.01 | 37.4 ±0.01 | 42.5±0.01 |
| Haematite relict | 12.5 ± 0.01 | 9.1 ±0.01 | 4.6 ± 0.02 |
| Haematite rhombic | 7.5 ± 0.01 | 6.4 ±0.01 | 4.1 ±0.01 |
| Haematite finely granular | 0.8 ± 0.02 | 0.5 ±0.01 | 0.2 ±0.01 |
| Haematite skeletal | 4.7 ± 0.01 | 4.0 ± 0.02 | 4.7 ± 0.02 |
| Haematite late stage | 0.8 ± 0.01 | 1.4 ± 0.01 | 2.1 ±0.01 |
| Total haematite | 26.3 ± 0.01 | 21.4 ± 0.02 | 15.7 ±0.01 |
| SFCA acicular | 13.1 ± 0.01 | 10.2 ±0.01 | 8.2 ± 0.01 |
| SFCA columnar and blocky | 15.1 ± 0.01 | 12.7 ±0.01 | 10.8 ±0.01 |
| SFCA dendritic and eutectic | 5.9 ± 0.01 | 8.3 ± 0.01 | 9.3 ± 0.02 |
| Total SFCA | 34.1 ± 0.02 | 31.2 ±0.01 | 28.3 ±0.01 |
| SFCA acicular/columnar | 0.87 | 0.80 | 0.76 |
| MO/(Fe,Mg)O | 1.2 ± 0.01 | 2.1 ±0.01 | 4.2 ±0.01 |
| Crystalline silicates | 5.8 ± 0.01 | 4.7 ±0.01 | 3.6 ±0.01 |
| Glass | 3.9 ± 0.01 | 4.3 ±0.01 | 6.8 ±0.01 |

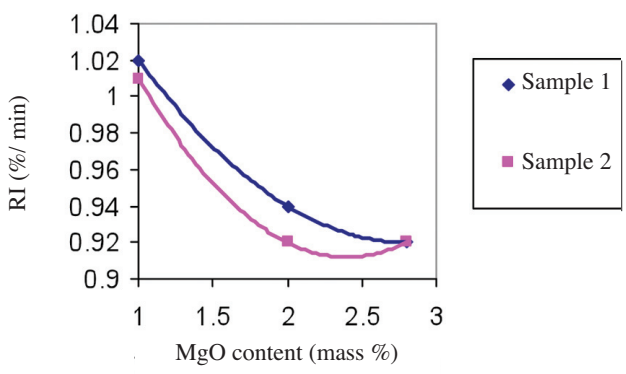


**Figure 1—Influence of MgO content on the reducibility index (low silica-low alumina sinter)**

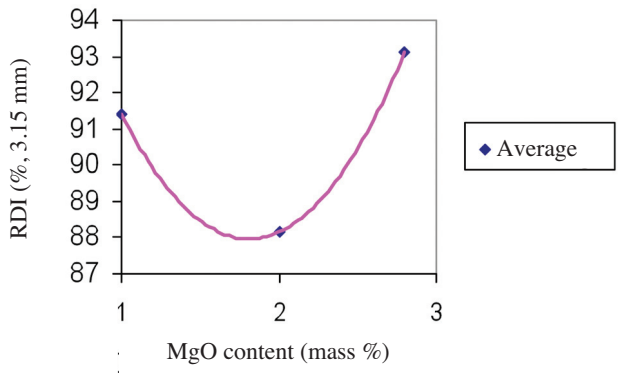


**Figure 2a—Variation of RDI (+3.15 mm) with MgO content (low silica-low alumina sinter)**

### *High silica-low alumina sinter*

*Mineralogy*

The phase compositions of the high silica-low alumina sinters are given in Table VI. It is clear that the volume percentage of the spinel phase increased with increasing MgO content while the total haematite decreased with increasing MgO. The volume percentage of spinel is slightly higher, and the volume percentage of haematite slightly lower, when fused magnesia was added as a source of MgO than when dolomite was added.

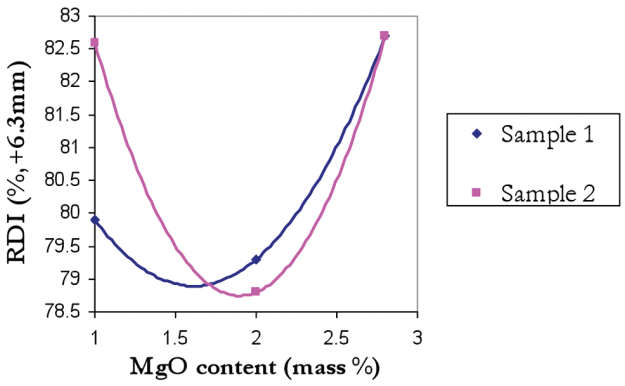


**Figure 2b—Variation of RDI (+6.3 mm) with MgO content (low silica-low alumina sinter)**

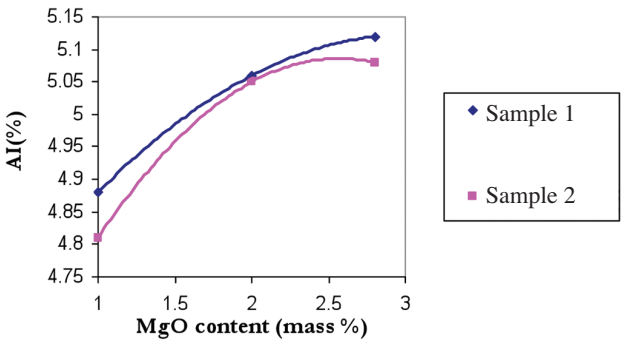


**Figure 3—Variation of abrasion index with MgO content (low silica-low alumina sinter)**

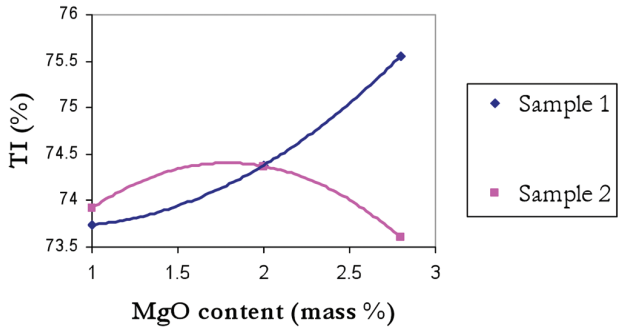


**Figure 4—Variation of tumbler index with MgO content (low silica—low alumina sinter)**

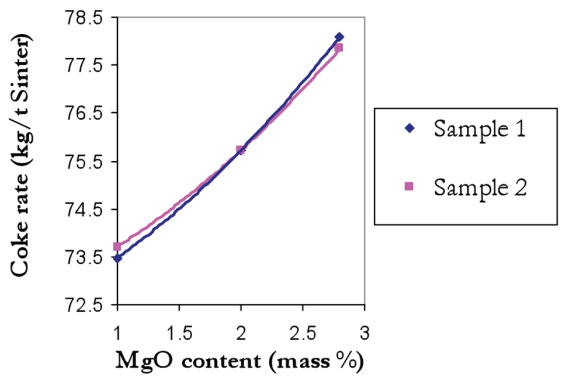


**Figure 5—Influence of MgO content of the sinter on coke breeze rate (low silica-low alumina sinter)**

*Table VI*

**Quantification of phases in the high silica-low alumina sinter (volume %)**

| Phase | MgO (mass%) | | | | | |
|---|---|---|---|---|---|---|
| | 1 | | 2 | | 2.8 | |
| | FM | Dolo | FM | Dolo | FM | Dolo |
| Spinel | 31.2±0.01 | 31.3±0.01 | 38.7±0.01 | 37.0±0.01 | 43±0.01 | 41.2±0.01 |
| Haematite relict | 12.3±0.02 | 13.4±0.01 | 11.2±0.01 | 14.2±0.01 | 1.6±0.01 | 2.0±0.01 |
| Haematite rhombic | 4.2±0.01 | 4.9±0.02 | 1.4±0.01 | 1.5±0.01 | 3.1±0.01 | 3.3±0.01 |
| Haematite finely granular | 1.2±0.01 | 1.4±0.01 | 0.1±0.02 | 1.0±0.01 | 0.1±0.01 | 1.8±0.01 |
| Hematite skeletal | 8.5±0.02 | 7.2±0.01 | 5.40±0.01 | 4.0±0.02 | 7.8±0.02 | 6.7±0.02 |
| Total Haematite | 26.2±0.02 | 26.9±0.01 | 17.9±0.01 | 20.7±0.01 | 12.6±0.02 | 13.8±0.01 |
| SFCA acicular | 7.5±0.01 | 7.9±0.02 | 5.2±0.02 | 8.8±0.02 | 5.6±0.01 | 5.8±0.01 |
| SFCA columnar and blocky | 14.9±0.01 | 15.1±0.01 | 13.6±0.02 | 20.0±0.02 | 11±0.01 | 14.6±0.01 |
| SFCA dendritic and eutectic | 12.9±0.01 | 13.1±0.01 | 11.8±0.01 | 5.4±0.01 | 10±0.01 | 12.7±0.01 |
| Total SFCA | 35.3±0.02 | 36.1±0.02 | 30.6±0.01 | 34.2±0.02 | 26.6±0.01 | 33±0.01 |
| SFCA: acicular/columnar ratio | 0.50 | 0.52 | 0.38 | 0.44 | 0.51 | 0.40 |
| MO/(Fe,Mg)O | 0.3±0.01 | 0.2±0.02 | 0.4±0.02 | 0.2±0.01 | 0.7±0.01 | 0.7±0.02 |
| Crystalline silicates | 3.6±0.01 | 5.4±0.01 | 4.9±0.01 | 5.5±0.01 | 5.6±0.01 | 6.0±0.01 |
| Glass | 3.0±0.01 | 2.7±0.01 | 3.2±0.01 | 3.2±0.01 | 4.8±0.01 | 5.8±0.01 |

FM = Fused Magnesia  Dolo = Dolomite

## Investigation into how the magnesia, silica, and alumina contents

The total amount of SFCA decreased with increasing MgO content in both types of sinters. However, more SFCA was produced with dolomite addition, whereas the columnar and blocky SFCA content of the sinter to which dolomite was added, was significantly higher than in the sinter to which fused magnesia was added. The higher amount of SFCA in the sinter where MgO was added as dolomite is presumably due to the fact that higher concentrations of SFCA form at lower temperatures (due to the decomposition of the carbonates that lower the sintering temperature) than at higher temperatures (with fused magnesia addition).

The (Fe,Mg)O phase, crystalline silicates, and glassy phase all increased with MgO content of the sinter, whereas more crystalline silicates were formed with dolomite addition.

*Sinter properties*

The reducibility of the sinters to which fused magnesia was added decreased when the MgO content increased from 1 to 2 mass per cent, and then increased when the MgO content increased to 2.8 mass per cent (Figure 6a). When the MgO was added as dolomite, the RI increased with increasing MgO content (Figure 6b). The values for the reducibility index obtained for the high silica sinters are lower than those obtained for the low silica sinters. The slightly higher $SiO_2$ content of the high silica-high alumina sinter has the effect of increasing the reducibility index of the sinter as the MgO content increased, whereas in the case of the low silica sinter the reducibility decreased with increasing MgO content. The values of the reducibility index obtained when MgO was added through dolomite addition were higher than those obtained with fused magnesia. This can be explained from the fact that lower sintering temperatures and higher oxygen partial pressures (due to $CO_2$ that was evolved) are associated with the sinter to which dolomite was added, and this caused lower concentrations of spinel, higher concentrations of total haematite, and higher concentrations of SFCA to form.

The influence of increasing MgO content on RDI (+3.15 mm) and RDI(+6.3 mm) are shown in Figures 7a and 7b for sinters to which fused magnesia was added, and Figures 8a and 8b for sinters to which dolomite was added. The RDI(+3.15 mm) and RDI(+6.3 mm) of the sinters where MgO was added in the form of fused magnesia increased only when the MgO content increased from 2 to 2.8 mass per cent, whereas with dolomite addition the reduction degradation indexes decreased with increasing MgO content.

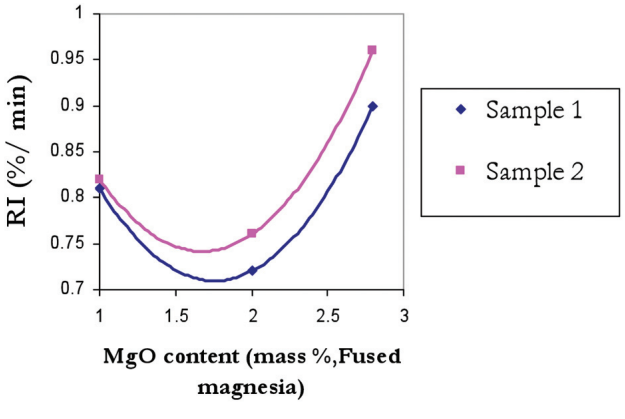


**Figure 6a—Variation of reducibility index (RI) with MgO (fused magnesia addition, high silica-low alumina sinter)**

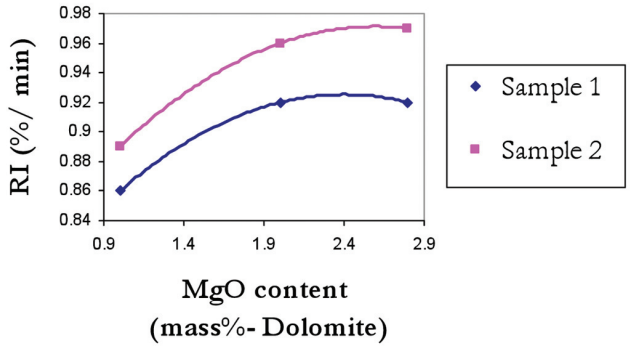


**Figure 6b—Variation of reducibility index (RI) with MgO (dolomite addition, high silica-low alumina sinter)**

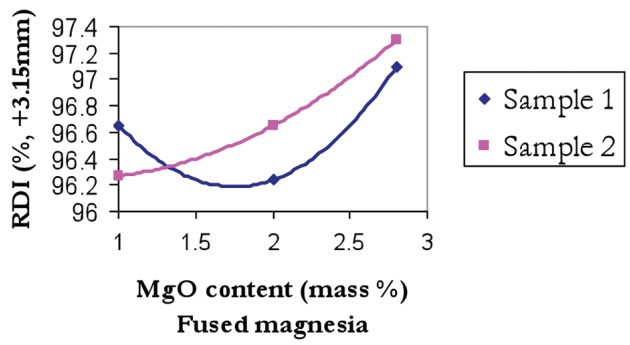


**Figure 7a—Influence of MgO content on the RDI (+3.15 mm) (fused magnesia addition, high silica-low alumina sinter)**

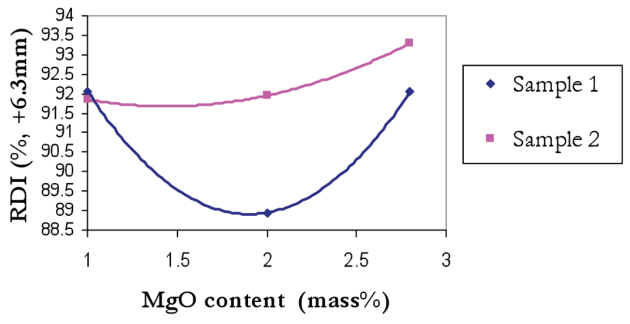


**Figure 7b—Influence of MgO content on the RDI (+6.3 mm) (fused magnesia addition, high silica-low alumina sinter)**

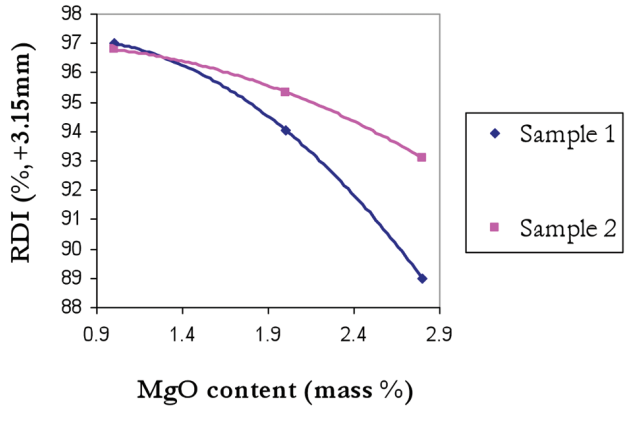


**Figure 8a—Influence of MgO content on the RDI (+3.15 mm) (dolomite addition, high silica-low alumina sinter)**

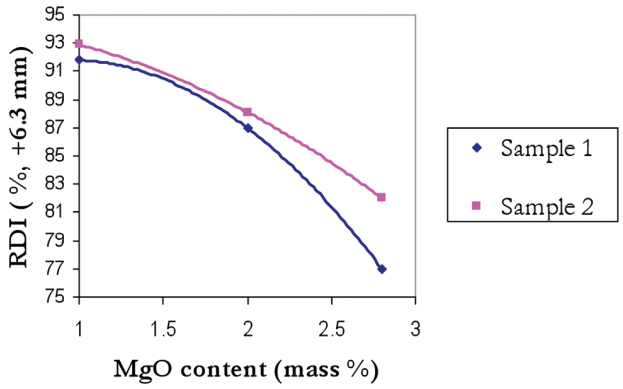


**Figure 8b—Influence of MgO content on the RDI (+6.3 mm) (dolomite addition, high silica-low alumina sinter)**

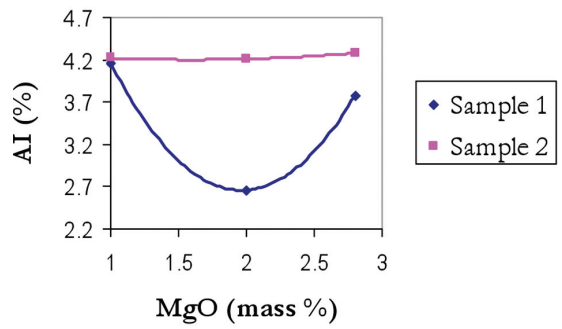


**Figure 9a—Influence of MgO content of the sinter on the AI (fused magnesia addition, high silica-low alumina sinter)**

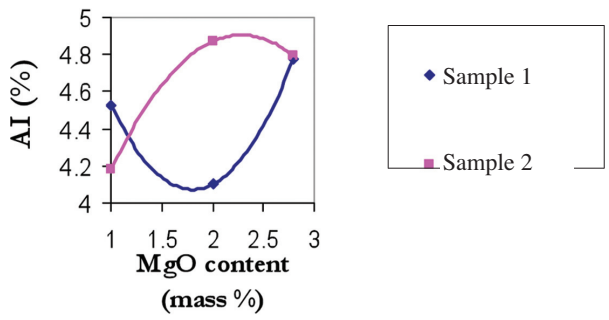


**Figure 9b—Influence of MgO content of the sinter on the AI (dolomite addition, high silica-low alumina sinter)**

The influence of MgO on the abrasion index of the sinters to which fused magnesia and dolomite were respectively added as MgO-bearing materials is shown in Figures 9a and 9b. The trends of the abrasion index were not the same for the sinter produced where the MgO content was increased through dolomite addition and through fused magnesia addition. The abrasion index of the sinter to which dolomite was added increased with increasing MgO content of the sinter (similar to what was observed in the low silica-low alumina sinter), whereas when fused magnesia was added the abrasion index first decreased and then increased with increasing MgO content. Values for the abrasion index were lower for the sinters in which the MgO content was increased through fused magnesia addition, than through dolomite addition.

The influence of MgO content of the sinter on the tumble index when fused magnesia and dolomite were respectively added is shown in Figures 10a and 10b. With the addition of fused magnesia the tumble index first decreased when the MgO content was increased to 2 mass per cent, after which it increased when the MgO content was further increased to 2.8 mass per cent. The addition of dolomite had the opposite effect: the tumble index increased slightly when the MgO content was increased to 2 mass per cent, after which it decreased when the MgO content increased to 2.8 mass per cent. Higher AI and lower TI values are associated with the sinters to which dolomite was added, which indicates that more fine material is associated with the sinters that were produced from dolomite than from fused magnesia.

The coke breeze rate increased with increasing MgO content of the sinters, and is higher for the sinters where the MgO content was increased through dolomite addition (Figure 11). This is due to more energy that is required to decompose the carbonates and dehydrate any $Ca(OH)_2$ and $Mg(OH)_2$.

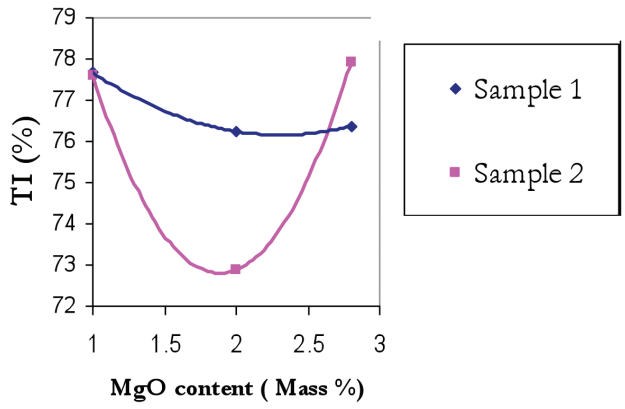


**Figure 10a—Influence of MgO content on TI (fused magnesia addition, high silica-low alumina sinter)**

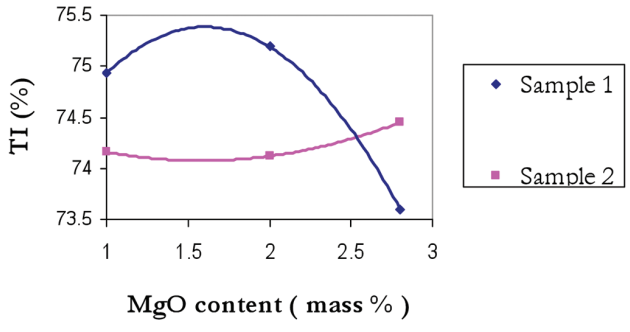


**Figure 10b—Influence of MgO content on TI (dolomite addition, high silica-low alumina sinter)**

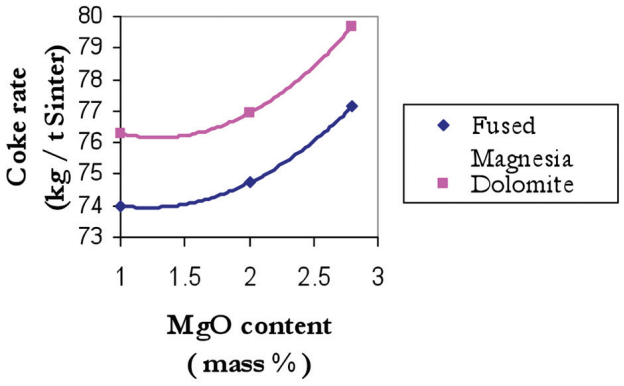


**Figure 11—Influence of MgO content on the coke breeze rate (high silica-low alumina sinter)**

### *High silica-high alumina sinter*

*Mineralogy*

The phase composition of the high silica-high alumina sinter is given in Table VII. The spinel as well as relict and total haematite contents in this sinter is lower than that obtained in the 2.8 per cent MgO (dolomite)-low silica-low alumina sinter, as well as the 2.8 mass per cent MgO-high silica-low alumina sinters. The acicular, columnar and total SFCA contents of this sinter is substantially higher than what was found for the 2.8 mass per cent MgO-low silica-low alumina and 2.8 mass per cent MgO (dolomite)-high silica-low alumina sinters, although the acicular/columnar SFCA ratio is similar to that of the 2.8 mass per cent MgO-high silica-low alumina sinter. The amount of crystalline silicates is similar to the 2.8 mass per cent MgO-low silica-low alumina sinter, but lower than the 2.8 mass per cent MgO-high silica-low alumina sinter. This 2.8 mass per cent MgO-high silica-high alumina sinter has the lowest glass content of all the examined sinters.

*Sinter properties*

The reducibility index of this high silica-high alumina sinter was 0.7, which is the lowest of the sinters that were studied, and less than the minimum of 1 per cent/min that is required by Kumba Iron Ore (Table VIII). The reduction degradation index (RDI(+6.3 mm)) was 74.6 per cent. Although it met the requirement of Kumba Iron Ore of ≥ 70 per cent, it has the lowest value of all the sinters produced. The abrasion index is 4.35 per cent, which is lower than the AI for both the 2.8 mass per cent MgO (dolomite)-low silica-low alumina and 2.8 mass per cent MgO (dolomite)-high silica-low alumina sinter. The tumble index of 66.4 per cent is the lowest observed in this study, and less than the minimum requirement of 70 per cent. The coke rate of 87.3 kg/t sinter is the highest of all the sinters produced in this project.

## Discussion

### *Effect of MgO content on mineralogy and properties*

Increasing the MgO contents from 1 to 3 mass per cent in the sinter (while keeping the $SiO_2$ and $Al_2O_3$ contents constant) increased the amount of spinel and glass, while it decreased the amounts of total and relict haematite, as well as total SFCA.

The AI, TI, and coke rate increased with increasing MgO content in the low silica-low alumina sinter, while the RI decreased. Both the RDI(+3.15 mm) and RDI(+6.3 mm) first decreased with an increase in MgO content from 1 to 2 mass per cent in the low silica-low alumina sinter, after which it increased when the MgO content was increased to 2.8 mass per cent.

In the case of the high silica-low alumina sinter, the form in which the MgO was added, had a pronounced effect on the majority of sinter properties. Only the coke rate increased with increasing MgO content in these sinters, irrespective of whether dolomite or fused magnesia was added. The coke rate was, however, higher for the sinters produced from dolomite than from fused magnesia. When MgO was added in the form of dolomite the AI and RI increased with increasing MgO content, whereas the TI first increased when the MgO content increased from 1 to 2 mass per cent MgO, after which it decreased when the MgO content further increased to 2.8 mass per cent. With fused magnesia addition the AI, TI, RI, RDI(+6.3 mm) decreased when the MgO content increased from 1 to 2 mass per cent, after which it increased with a further addition of MgO to 2.8 mass per cent.

### *Effect of $SiO_2$ content on mineralogy and properties*

When the $SiO_2$ content of the sinter was increased from 5.1 to

*Table VII*

**Quantification of phases of the high silica-high alumina sinter**

| Phase | Volume % |
|---|---|
| Spinel | 35.5±0.01 |
| Haematite relict | 1.3±0.01 |
| Haematite rhombic | 4.4±0.01 |
| Haematite finely granular | 2.4±0.01 |
| Haematite skeletal | 3.8±0.02 |
| Total haematite | 11.9±0.01 |
| SFCA acicular | 11.3±0.01 |
| SFCA columnar and blocky | 25.4±0.01 |
| SFCA dendritic and eutectic | 4.1±0.02 |
| Total SFCA | 40.8±0.02 |
| MO/(Mg,Fe)O | 3.2±0.01 |
| Periclase | 0.3±0.01 |
| Crystalline silicates | 3.5±0.01 |
| Glass | 4.4±0.01 |
| Comment: SFCA acic/col. | 0.44 |

*Table VIII*

**Sinter properties of the high silica-high alumina sinter**

| RI (%/min) | RDI (%) | | AI (%) | TI (%) | Coke rate (Kg/t sinter) |
|---|---|---|---|---|---|
| | +3.15 mm | +6.3 mm | | | |
| 0.7 | 89.9 | 74.6 | 4.35 | 66.4 | 87.32 |

5.7 mass per cent (while keeping the $Al_2O_3$ and MgO contents constant) the amount of spinel and total haematite remained virtually unchanged, while the total amount of SFCA increased and the glassy phase decreased with increasing MgO contents. The amount of crystalline silicates also increased with increasing $SiO_2$ content, but only for 2 and 2.8 mass per cent MgO.

The RI decreased with increasing $SiO_2$ content, only in the case of the 1 mass per cent MgO sinter, whereas for 2 and 2.8 mass per cent MgO it remained virtually constant. Both the RDI(+3.15 mm) and RDI(+6.3 mm) increased with increasing $SiO_2$ content for sinters that contained 1 and 2 mass per cent MgO, and decreased with a further increase in MgO content to 2.8 mass per cent. The AI decreased with increasing $SiO_2$ content in all the examined sinters, whereas the TI increased with increasing $SiO_2$ content in the 1 and 2 mass per cent MgO sinters, and decreased in the 2.8 mass per cent MgO sinter. The coke rate increased with increasing $SiO_2$ content in all the studied sinters.

### *Effect of $Al_2O_3$ content on mineralogy and properties*

Increasing the $Al_2O_3$ content of the sinter from 1.7 to 2.9 mass per cent (while keeping the $SiO_2$ and MgO contents constant) increased the acicular, columnar and blocky, as well as total amount of SFCA, while decreasing all other phases (i.e. spinel, total haematite, crystalline silicates, and glass, along with dendritic and eutectic SFCA).

Increasing $Al_2O_3$ contents decreased the AI, TI, RI, RDI(+3.15 mm) as well as RDI(+6.3 mm) of the sinter.

### *Dolomite vs. fused magnesia addition*

Although the addition of fused MgO as a flux to iron sinter is not a viable option, these test results confirmed that the form in which fluxes are added to the raw material mixture, influence the mineralogy and properties of the produced sinter. Since heat is required to decompose the dolomite, and any hydroxides that may form, it can be assumed that the sintering temperatures associated with dolomite addition were lower than with fused magnesia addition, and oxygen partials pressures higher due to $CO_2$ evolution.

Dolomite addition favoured higher concentrations of relict haematite, total SFCA and crystalline silicates in all the examined sinters, and higher acicular/columnar SFCA ratios when the sinters contained 1 and 2 mass per cent MgO. Fused magnesia addition in turn favoured spinel formation in the 2 and 2.8 mass per cent MgO sinters.

Dolomite addition to the high silica-low alumina sinter favoured the RI, RDI(+3.15 mm) and RDI(+6.3 mm) at 1 mass per cent MgO. Fused magnesia addition, however, favoured the RDI(+3.15 mm) and RDI(+6.3 mm) of the sinters that contained 2 and 2.8 mass per cent MgO, as well as the AI and TI.

## Conclusions

- The mineralogy of iron sinter can more easily be predicted from its chemical composition than its physical and chemical properties. Increasing MgO concentrations in the sinter increases the amounts of the spinel and glassy phases, while increasing $SiO_2$ concentrations in the sinter increases the amount of total SFCA, decreases the acicular/columnar SFCA ratio and glassy phase content, while increasing the crystalline silicate content at MgO concentrations of 2 and 2.8 mass%. Increasing $Al_2O_3$ contents in the sinter resulted in a sinter with a substantially higher concentration of the SFCA phase. The amount of acicular, columnar and blocky SFCA increased significantly, although a substantial reduction in the amount of dendritic and eutectic SFCA was detected.
- The MgO and $SiO_2$ contents of iron sinter seem to have an interrelated effect on its physical and chemical properties. Predicting the effect that varying amounts of MgO and $SiO_2$ would have on sinter properties is therefore complex. The only clear trends are the AI which increases with increasing MgO content, and the RI and AI of the sinter which decrease with increasing $SiO_2$ content of the sinter.
- Increasing $Al_2O_3$ contents in the sinter resulted in a drastic deterioration in its chemical and physical properties, although the concentration of the SFCA phase increased. The role of the SFCA phase in producing a sinter of high quality is therefore not yet fully understood.
- The mineral form in which fluxes are added to the raw material sinter mixture (e.g. oxide vs. carbonate) have a pronounced effect on the mineralogy and properties of the produced sinter.

## Acknowledgements

The authors would like to thank the Value In Use Group, Kumba Iron Ore for financial and technical support.

## References

1. Hsieh, L.H. and Whiteman, J.A. Sintering conditions for simulating the formation of mineral phases in industrial iron ore sinter. *ISIJ International*, 1989. vol. 29, pp. 24–32.
2. Chaigneau, R. and Heerema, R.H. Calcium ferrites and the diversity in their reduction behaviour. *Ironmaking Conference Proceedings*, Toronto, 1992. pp. 111–120.
3. Egundebi, G.O. and Whiteman, J.A. Evolution of microstructure in iron ore sinter. *Ironmaking and Steelmaking*, 1989. vol. 16, pp. 379–385.
4. Pal, S., Chandra, N., Mishra, U.N., Singh, R.N., and Mediratta, S.R. Effect of mineralogical composition of iron-bearing materials on softening-melting properties. *CSTI Ironmaking Conference Proceedings*, 1998. pp. 1615–1635.
5. Hsieh, L.H. Effect of raw material composition on the sintering properties. *ISIJ International,* 2005. vol. 45, pp. 551–559.
6. Choudary, M.K. and Nandy, B. Effect of flame front speed on sinter structure of high alumina iron ores. *ISIJ International.* 2006, vol. 46, pp. 611–613.
7. Pimenta, H.P. and Seshadri, V. Characterisation of structure of iron ore sinter and its behaviour during reduction at low temperatures. *Iron and Steelmaking*, 2002. vol. 29, pp. 169–174.
8. Bristow, N.J. and Waters, A.G. Role of SFCA in promoting high-temperature reduction properties of iron ore sinters. *Mineral Processing and Extractive Metallurgy* (Trans. IMM C), 1991. vol.100, pp. C1–C10.
9. Maeda, T., Nishioka, K., Nakashima, K., and Shimizu, M. Formation rate of calcium ferrite melt focusing on $SiO_2$ and $Al_2O_3$ components. *ISIJ International*, 2004. vol. 44, pp. 2046–2051.

10. Higuchi, K., Naito, M., Nakano, M., and Takamoto, Y. Optimization of chemical composition on microstructure of iron ore sinter for low-temperature drip of molten iron with high permeability. *ISIJ International*, 2004. vol. 44, pp. 2057–2066.
11. Loo, C.E. and Leung, W. Factors influencing the bonding phase structure of iron ore sinters. *ISIJ International*, 2003. vol. 43, pp. 1393–1402.
12. Machida, S., Mushiro, K., Ichikawa, K., Noda, H., and Sakai, H. Experimental evaluation of chemical composition and viscosity of melts during iron ore sintering. *ISIJ International*, 2005. vol. 45, pp. 513–521.
13. Pownceby, M.I. and Clout, J.M.F. Importance of fine ore chemical composition and high temperature phase relations: Applications to iron ore sintering and pelletising. *Mineral Processing and Extractive Metallurgy* (Trans. IMM C), 2003. vol. 12, pp. 44–51.
14. Matsumura, M., Hoshi, M., and Kawaguchi, T. Improvement of sinter softening property and reducibility by controlling chemical compositions. *ISIJ International*, 2005. vol. 45, pp. 594–602.
15. Goldring, D.C., Jukes, L.M., and Fray, T.A.T. Characterisation of Iron Ore Sinter from its Mineralogy. *Institute of Chemical Engineers*, *5th International Symposium on Agglomeration*, Brighton, UK, 25–27 September 1989. pp. 425–429.
16. Kasai, E., Rankin, W.J., Lovel, R.R., and Omori, Y. An Analysis of the Structure of Iron Ore Sinter Cake, *ISIJ International*, 1989. vol. 29, pp. 635- 641. ◆